

Safety of intradiscal injection and biocompatibility of polyester amide microspheres in a canine model predisposed to intervertebral disc degeneration

Nicole Willems,¹ George Mihov,² Guy C.M. Grinwis,³ Maarten van Dijk,² Detlef Schumann,² Clemens Bos,⁴ Gustav J. Strijkers,⁵ Wouter J.A. Dhert,^{1,6} Björn P. Meij,¹ Laura B. Creemers,⁶ Marianna A. Tryfonidou¹

¹Department of Clinical Sciences of Companion Animals, Faculty of Veterinary Medicine, 3584 CM Utrecht, The Netherlands

²R&D Orthopedics, DSM Biomedical materials B.V., 6167, RA, Geleen, The Netherlands

³Department of Pathobiology, Faculty of Veterinary Medicine, 3508 TD Utrecht, The Netherlands

⁴Imaging Division, University Medical Center, 3584 CX, Utrecht, The Netherlands

⁵Biomedical Engineering and Physics, Academic Medical Center (AMC), 1100 DE, Amsterdam, The Netherlands

⁶Department of Orthopaedics, University Medical Center, 3584 CX, Utrecht, The Netherlands

Received 28 August 2015; revised 30 October 2015; accepted 18 November 2015

Published online 21 December 2015 in Wiley Online Library (wileyonlinelibrary.com). DOI: 10.1002/jbm.b.33579

Abstract: Repair of degenerated intervertebral discs (IVD) might be established via intradiscal delivery of biologic therapies. Polyester amide polymers (PEA) were evaluated for *in vitro* cytotoxicity and *in vivo* biocompatibility, and thereafter intradiscal application of PEA microspheres (PEAMs) in a canine model predisposed to IVD degeneration at long-term (6 months) follow-up. PEA extracts did not induce cytotoxicity in mouse fibroblast cells (microscopy and XTT assay), while a slight foreign body reaction was demonstrated by histopathology after intramuscular implantation in rabbits. Intradiscal injection of a volume of 40 μ L through 26 and 27G needles induced no degenerative changes in a canine model susceptible to IVD disease. Although sham-injected IVDs showed increased *CAV1* expression compared with noninjected IVDs, which may indicate increased cell senescence,

these findings were not supported by immunohistochemistry, biomolecular analysis of genes related to apoptosis, biochemical and histopathological results. PEAM-injected IVDs showed significantly higher *BAX/BCL2* ratio vs sham-injected IVDs suggestive of an anti-apoptotic effect of the PEAMs. These findings were not supported by other analyses (clinical signs, disc height index, T2 values, biomolecular and biochemical analyses, and IVD histopathology). PEAs showed a good cytocompatibility and biocompatibility. PEAMs are considered safe sustained release systems for intradiscal delivery of biological treatments. © 2015 Wiley Periodicals, Inc. *J Biomed Mater Res Part B: Appl Biomater*, 105B: 707–714, 2017.

Key Words: dog, biomaterial, microspheres, nucleus pulposus, intradiscal delivery

How to cite this article: Willems N, Mihov G, Grinwis GCM, van Dijk M, Schumann D, Bos C, Strijkers GJ, Dhert WJA, Meij BP, Creemers LB, Tryfonidou MA. 2017. Safety of intradiscal injection and biocompatibility of polyester amide microspheres in a canine model predisposed to intervertebral disc degeneration. *J Biomed Mater Res Part B* 2017;105B:707–714.

INTRODUCTION

Intervertebral disc (IVD) disease is common in dogs and humans and is associated with IVD degeneration. The process of spontaneous IVD degeneration in chondrodystrophic dogs is similar to that in man, resulting in a valuable animal model for canine and human patients.¹ Clinical signs, i.e. pain, neurological deficits, develop from an age of 3–7 years in these dogs. An aberrant cell-mediated response, associated with genetic predisposition, aging, mechanical overload, and an inadequate metabolite transport results in an imbalance between anabolic and catabolic processes and consequently a dysfunctional extracellular matrix (ECM).² The nucleus pulposus (NP) and inner annulus fibrosus (AF), nor-

mally consisting of mainly collagen type II and large proteoglycan aggregates, change to tissues rich in collagen type I, with a decrease in the size and total amount of proteoglycans, while the fibrils of the outer AF become coarser and more susceptible to injury. These changes ultimately result in disturbance of the structural integrity and biomechanical properties of the IVD.²

With increased knowledge on the pathogenesis and biological changes in the diseased IVD, treatment strategies focus on biological repair of the IVD. As the IVD is the largest avascular structure of the body,³ direct intradiscal injection via a minimal invasive technique is an elegant way to deliver biological treatments, e.g. cells, growth factors or

Additional Supporting Information may be found in the online version of this article.

Disclosure: The authors declare that they have no competing interests.

Correspondence to: M.A. Tryfonidou; e-mail: m.a.tryfonidou@uu.nl

drugs, into the NP. Growth factors are characterized by short *in vivo* half-lives and chemical instability and to increase their bioavailability *in vivo*, bioactive substances can be encapsulated in biomaterials, e.g. microspheres, hydrogels, that allow sustained release.⁴ In addition, higher loading doses can be achieved locally, without causing systemic side effects, and puncture of the IVD can be reduced to a minimum.

A class of polyester amide polymers (PEAs) have gained interest as biodegradable polymers in the past decades, as they possess clear advantages over aliphatic polyester-based biomaterials commonly used.^{5,6} The latter are rather hydrophobic, hydrolytically degradable, and most of them generate acidic products upon degradation. In contrast, PEAs are synthetic, amino-acid-based co-polymers, containing L-amino acids, aliphatic di-carboxylic acids, and α,ω -diols, creating amphiphilicity, that enhances interactions with proteins and modification with bioactive molecules and (lipophilic) drugs.^{7,8} Biodegradation of the polymers occurs via surface erosion, and can be accomplished by endogenous enzymes.^{9,10} PEAs can be manufactured by a polycondensation method and mechanical and thermal properties can be easily tuned.⁸ They have been successfully applied as a coating on coronary stents for sustained drug release,^{11,12} and were proven to meet the requirements of a biocompatible controlled release system in the ocular environment.^{13,14} To our knowledge, the intradiscal application of microspheres consisting of PEAs, has not been examined thus far, and seems a promising method to provide sustained release of bioactive substances over a prolonged period in the confined environment of the IVD.

Intradiscal application of therapeutics should be considered with care. In animal models of IVD degeneration, puncture of the IVD induces degeneration, and the gauge size of the needle correlates with the extent of degeneration.¹⁵⁻¹⁷ Also, a relatively high volume applied intradiscally can cause an increase in hydrostatic pressure, a biomechanical cue shown to induce IVD degeneration.^{18,19} Furthermore, in human patients, discography injections have been associated with an increased risk of degeneration. As several ongoing clinical trials on intradiscal delivery of biologic therapies are performed (<http://clinicaltrials.gov>), it is important to assess possible side effects of intradiscal injection to pinpoint the boundary conditions. *In vivo* assessment of safety and efficacy of treatments in clinical trials is obviously limited to radiography and magnetic resonance imaging, which may not be sensitive enough to detect minor changes in the ECM that may have clinically relevant effects on the long term. Assessment of the effect of intradiscal injection at a biochemical, biomolecular, and histopathological level will provide much more information. Preferably this is done in a large animal model with spontaneous IVD degeneration, where underlying pathological processes match human IVD degeneration providing valuable translational information.¹ In order to assess the effects of intradiscal injection of a sham condition in IVDs in dogs predisposed to IVD degeneration, we evaluated magnetic resonance imaging (MRI), in combination with biochemical, biomolecular, and histopatho-

logical data at long-term follow-up (6 months). Furthermore, after evaluating the biocompatibility and safety of intramuscular application of PEAs in rabbits, we also evaluated the long-term effects on IVD integrity of PEA microspheres (PEAMs) after intradiscal application (6 months).

MATERIALS AND METHODS

Ethics statement

All procedures involving animals were approved and conducted according to US regulation (rabbits), and to Dutch regulation (dogs; experimental number: 2012.III.07.065). **Synthesis PEAs.** PEAs were synthesized according to a previously published method.^{13,20} Briefly, the polymer was prepared via polycondensation of 0.45 equivalents of di-*p*-toluenesulfonic acid salts of bis-(L-leucine)1,4-dianhydrosorbitol diester (1), 0.30 equivalents of bis-(L-leucine) α,ω -hexanediol diester (2), 0.25 equivalents of lysine benzyl ester (3), and 1 equivalent of di-N-hydroxysuccinimide ester of sebacic acid (4) in anhydrous dimethylformamide and trimethylamine in a glass vessel with overhead stirrer under a nitrogen atmosphere. Employing pre-activated acid in the reaction allows polymerization at a relative low temperature (65°C), resulting in a polycondensate free of by-products and predictable degradation components. The polymer with an average number molecular weight of 48 kDa was isolated from the reaction mixture in two precipitation steps.

Preparation of PEA microspheres (PEAMs)

A volume of 30 mL of 1% filtered polyvinyl alcohol (PVA) was stirred with an Ultra-Turrax® (IKA Labortechnik, Staufen, Germany) equipped with a 25S-10G stirring rod) at 4000 rpm. A volume of 150 μ L of 10% trehalose in water was added to 8.5% polymer in dichloromethane (DCM) and vortexed for 30 s at 13,000 rpm. This emulsion was injected into the PVA solution and stirred at 4000 rpm. After 3 min the Ultra-Turrax was removed, a stirring bar was added and the emulsion was stirred for another 16 hours. After stirring, the PEAMs were allowed to sink to the bottom of the vial and the supernatant was removed. The PEAMs were washed three times with 20 mL of 0.04% ice-cold, filtered Tween® 20. Following the final washing about 5 mL of 0.04% Tween® 20 was added, and the PEAMs were lyophilized. The average diameter of the microspheres was 40 μ m.

In vitro cytotoxicity PEAs

For cytotoxicity testing, mouse L-929 fibroblast cells were cultured in high glucose Dulbecco's modified Eagle's medium (DMEM, Lonza, Verviers, Belgium) supplemented with 10% fetal bovine serum (FBS, Lonza), 1% penicillin/streptomycin (pen/strep), and plated into 96-well plates at a density of 9×10^3 cells/cm². Autoclaved natural rubber and silicone served as a positive and a negative control, respectively. Extractions of 4 g (surface \pm 60 cm²) of gamma-irradiated polymer specimens were prepared in 20 mL cell culture medium (MEM Eagle with Earle's BSS with L-glutamine, Lonza) 10% FBS + 1% pen/strep and subsequently incubated at 37°C for 24 h in a humidified atmosphere (5% CO₂). Cells were exposed to the PEA extracts or

controls at 37°C for 48 h (5% CO₂). Cell viability was immediately recorded by microscopic examination of the cells and by using the XTT assay.²¹ Cell viability assays were performed with three or more replicates.

Biocompatibility of PEAs in rabbits

Three healthy adult New Zealand White rabbits (Charles River, Wilmington, MA, USA) were fully anesthetized and six sterilized strips of PEAs of 1 x 1 x 10 mm in size were implanted into the paravertebral muscles under sterile conditions. Six strips of plastic served as a control. Rabbits were monitored daily for signs of distress or pain (e.g. lethargy, weight loss, automutilation, and abnormal posture) and injection sites were monitored for inflammation (e.g. swelling, redness, pain, and heat). After 2 weeks all animals were sacrificed. The implants were excised, macroscopically evaluated and fixed in 4% neutral buffered formaldehyde. Paraffin sections of 4 μm were stained with hematoxylin and eosin and histopathologically assessed for infiltration of inflammatory cells, giant cells, necrosis, neovascularization, fatty infiltration, and the encapsulation of the biomaterial by a fibrotic capsule.

Long-term (6-month) effect of intradiscal injection on canine IVDs

This study was performed in seven intact male beagle dogs (Harlan) with a median age of 1.3 years (range 1.1–1.8) and a median weight of 11.7 kg (range 10.2–12.8). A board-certified veterinary surgeon (BM) performed a general, orthopedic, and neurologic examination on all dogs. A blood sample was drawn from the jugular vein to assess white blood cell count and differentiation, to exclude systemic inflammation. T2-weighted images were obtained pre- (t_0) and postoperatively at 6 (t_6), 12 (t_{12}), and 24 (t_{24}) weeks under general anesthesia using a 1.5 Tesla scanner (Philips Healthcare, Best, The Netherlands).²² All lumbar IVDs were assessed at all four time points according to the Pfirrmann score, by a veterinary radiologist that was blinded to treatment allocation on sagittal T2-weighted images. Only lumbar IVDs with a Pfirrmann score II were included in the study. All injections were performed by the same person (BM), and noninjected IVDs served as controls. Briefly, T12–L5 were exposed and injected via a left lateral approach, and L6–S1 via a dorsal approach. A 100 μL gastight syringe (7656–01 Model 1710 RN) was used to inject 40 μL of a sham containing 1% sucrose, 1.2% mannitol, 20 mM glycine, and 0.05% Tween[®] 20 through a 27G needle (25 mm, 12° beveled point; Hamilton Company USA, Reno, Nevada, USA). A volume of 40 μL of 1.3% PEAMs in 0.9% NaCl needed to be injected through a 26G needle (25 mm, 12° beveled point; Hamilton) to avoid clogging by the microspheres (unpublished data). The choice for the sham was based on the intradiscal injection of three other substances unrelated to this study.²² Location of the tip of the needle in the NP was estimated by the length of passage through the AF (1 cm), while constant resistance was encountered. Once the NP was encountered, resistance decreased and the volume could be easily injected. The needle was slowly

pulled back to allow the AF puncture site to close, and the site was inspected for extrusion of the administered substance.

Disc height index (DHI) was calculated at all four time points on T2-weighted images.²² At all four time points, quantitative T2 maps were generated from a multi-echo imaging sequence with 8 echoes. For the analysis of T2 values in the NP, an oval-shaped region of interest (ROI) in the NP was manually placed on mid-sagittal IVD sections. ROIs were exported to, and analyzed with Wolfram Mathematica 10.0 (Wolfram Research, Champaign, IL, USA). T2 values were computed by calculating the mean signal intensity (S) in each ROI, and by fitting these intensity data to the following equation: $S(\text{TE}) = S_0 e^{-\text{TE}/T_2}$ using the Levenberg-Marquardt nonlinear least-squares method implemented in Mathematica. S_0 denotes the equilibrium magnetization, whereas $S(\text{TE})$ indicates the signal as a function of echo time (TE).

Sample collection, macroscopic grading, and histopathological grading of canine IVDs

Dogs were euthanized 6 months after intradiscal injection by way of sedation with dexmedetomidine followed by pentobarbital. The vertebral column (T12–S1) was harvested to generate nine spinal units.²² One part of the IVD tissue, containing both NP and AF, was snap frozen in liquid nitrogen and stored at –80°C for biochemical and biomolecular analyses. The other part was photographed (Olympus VR-340, Hamburg, Germany) for macroscopic evaluation, and fixed in 4% buffered formaldehyde at 4°C for 2 weeks. Two independent investigators, blinded to the treatments, evaluated macroscopic images of the IVD segments according to the Thompson grading scheme. Samples were decalcified according to Kristensen in 35% formic acid and 6.8% sodium formate.²³ Paraffin sections (5 μm) stained with hematoxylin/eosin and with picosirius red/alcan blue were histopathologically evaluated by two independent investigators, blinded to the treatments, according to the grading scheme developed by Bergknut et al.²⁴ Immunohistochemistry for caveolin-1 [monoclonal mouse anti-caveolin-1 antibody (Clone 2297, 610406, BD Biosciences) diluted 1:50 in PBS] was performed as described previously.²⁵

RNA isolation and qPCR of NP and AF. Transverse cryosections (60 μm) of the IVDs were collected and the NP and AF tissues were separated visually. One half was collected in 300 μL RLT buffer containing 1% β-mercapto-ethanol (Qiagen, Venlo, The Netherlands) and stored at –80°C until biomolecular analyses. Total RNA was isolated from the NP and AF tissues by using the RNeasy Fibrous Tissue Mini Kit (Qiagen, Venlo, The Netherlands) according to the manufacturer's instructions. The incubation period with proteinase K was reduced to 5 min increase RNA yield. After on-column DNase-I digestion (Qiagen RNase-free DNase kit), RNA was quantified by using a NanoDrop 1000 spectrophotometer (Isogen Life Science, IJsselstein, The Netherlands). The iScript[™] cDNA Synthesis Kit (Bio-Rad, Veenendaal, The Netherlands) was used to synthesize cDNA. Quantitative

PCR (qPCR) was performed using an iCycler CFX384 Touch thermal cycler, and IQ SYBRGreen Super mix (Bio-Rad) to assess the effects at gene expression levels with regards to: (1) ECM anabolism: *aggrecan (ACAN)*, *collagen type II (COL2A1)*, *collagen type I (COL1A1)*; (2) ECM catabolism: *a disintegrin and metalloproteinase with thrombospondin motifs (ADAMTS5)*, *matrix metalloproteinase 13 (MMP13)*, *tissue inhibitor of metalloproteinase 1 (TIMP1)*; (3) proliferation: *cyclin-D1 (CCND1)*, and (4) apoptosis: *caveolin-1 (CAV1)*, *caspase 3 (CASP3)*, and *B-cell lymphoma 2-associated X/B-cell lymphoma 2 (BAX/BCL2)* ratio (Supporting Information 1). Relative expression levels were determined by normalizing the C_t value of each target gene by the mean C_t value of four reference genes, i.e. *glyceraldehyde 3-phosphate dehydrogenase (GAPDH)*, *ribosomal protein S18 (RPS19)*, *succinate dehydrogenase complex, subunit A, flavoprotein variant (SDHA)*, and *hypoxanthine-guanine phosphoribosyltransferase (HPRT)*.

Biochemical assays: glycosaminoglycan (GAG), collagen and DNA. The other half of the cryosectioned NP and AF tissues was digested overnight in papain buffer (250 μ g/mL papain (P3125-100 mg, Sigma-Aldrich) + 1.57 mg/mL cysteine HCL (C7880, Sigma-Aldrich)) at 60°C. GAG content was quantified by using a 1,9-dimethylmethylene blue assay.²⁶ The Quant-iT™ dsDNA Broad-Range assay kit in combination with a Qubit™ fluorometer (Invitrogen, Carlsbad, USA) was used in accordance with the manufacturer's instructions. Collagen was quantified by using a hydroxyproline assay and calculated from the hydroxyproline content by multiplying with a factor 7.5.²⁷ Total GAG and collagen content were normalized for DNA content of the NP and AF.

STATISTICAL ANALYSIS

All data were analyzed by using *R* statistical software, package 3.0.2 (www.r-project.org). Residual plots and quantile-quantile (Q-Q)-plots were used to check normality of the data. In case of violation of the assumption of normality, data were logarithmically transformed. A linear mixed effect model was used to analyze the effect of intradiscal injection and intradiscal application of PEAMs on DHI, T2 values, histopathological grading, GAG, collagen, and DNA content. Model selection was based on the lowest Akaike Information Criterion (AIC). The correlation between multiple measurements within one dog was taken into account by incorporating "dog" (dog 1–7) as a random effect. DHI and T2 values were corrected for t_0 , and "treatment", "time" (t_6 , t_{12} , and t_{24}), and their interaction served as fixed effect factors. "Treatment" (noninjected, sham, PEAMs) served as a fixed factor in the analysis of histopathological scores. For the analysis of GAG and DNA levels, "treatment", "tissue" (NP and AF), and their interaction were incorporated into the model as fixed effect factors. The Cox proportional hazards regression model was used to estimate the effect of the injected treatments on gene expression levels. Calculations were performed on the ratio of the C_t values for each target gene to the mean C_t value of the reference genes. C_t values ≥ 40 were right censored. Regression coefficients were

estimated by the maximum likelihood method. Differences between treatments were considered significant if 0 was not included in the confidence interval, whereas hazard ratios were considered significant if 1 was not included in the confidence interval. Confidence intervals were calculated and stated at the 99% confidence level to correct for multiple comparisons.

RESULTS

Cytocompatibility of PEA *in vitro* and biocompatibility of PEA and PEAMs *in vivo*

No visible signs of toxicity in response to the PEAs were observed in the fibroblast monolayers at microscopic evaluation. Cell viability, as measured by the XTT assay, was 97.9% after 48 h incubation with PEA dispersions, and was considered noncytotoxic.²⁸ Macroscopic evaluation of the PEA implant sites in rabbits indicated no significant signs of inflammation, encapsulation, hemorrhage, necrosis, or discoloration after two weeks. Microscopic evaluation of the implant sites indicated no significant signs of fibrosis, hemorrhage, necrosis, or degeneration compared with the control implant sites. Cellular infiltrates and giant cells were seen at the interface of the test implant sites. Individual scores of the rabbits are shown in Supporting Information 2. Overall, implantation of PEA specimens demonstrated a slight foreign body reaction intramuscularly.

Intradiscal injection in a canine model of spontaneous IVD degeneration

All dogs recovered from surgery uneventfully. All 21 injected IVDs were scored a Pfirrmann grade II before surgery (t_0). Pfirrmann scores of 20/21 IVDs and T2-values of all IVDs were not significantly different over time (t_6 , t_{12} , t_{24}). T2-values per condition are described in Supporting Information 3. One (1/21) sham-injected IVD was scored a Pfirrmann grade III at all subsequent time points. The mean DHI of noninjected, sham-injected, and PEAMs-injected IVDs were not significantly different [Figure 1(A)]. Mean disc height of noninjected IVDs was 3.84 mm (range 3.20–4.93 mm). As the outer diameter of a 27G needle is 0.41 mm and of a 26G needle 0.47 mm, the ratios of needle diameter to disc height were calculated at 11% and 12%, respectively. The volume injected in this study consisted of 20% of the total NP volume (that is, 40 μ L of 200 mm³).²⁹ Postmortem, all IVDs were scored a Thompson grade II, in accordance with early IVD degeneration. Representative macroscopical images of all three conditions are shown in Figure 1(B–D).

Histopathology and biochemistry

The median histopathological grade of noninjected (12; range: 10–15), sham-injected (14; range: 11–17), and PEAMs-injected IVDs 13 (11–15) was not significantly different. Representative histopathological images (picrosirius red/alcian blue stain) of all conditions are shown in Figure 1(B', B'', C', C'', and D', D''). In one of the PEAMs-injected IVDs (level L7–S1) a small pyogranulomatous reaction in the dorsal ligament and outer layer of the dorsal AF was detected, indicative of an inflammatory response. GAG and

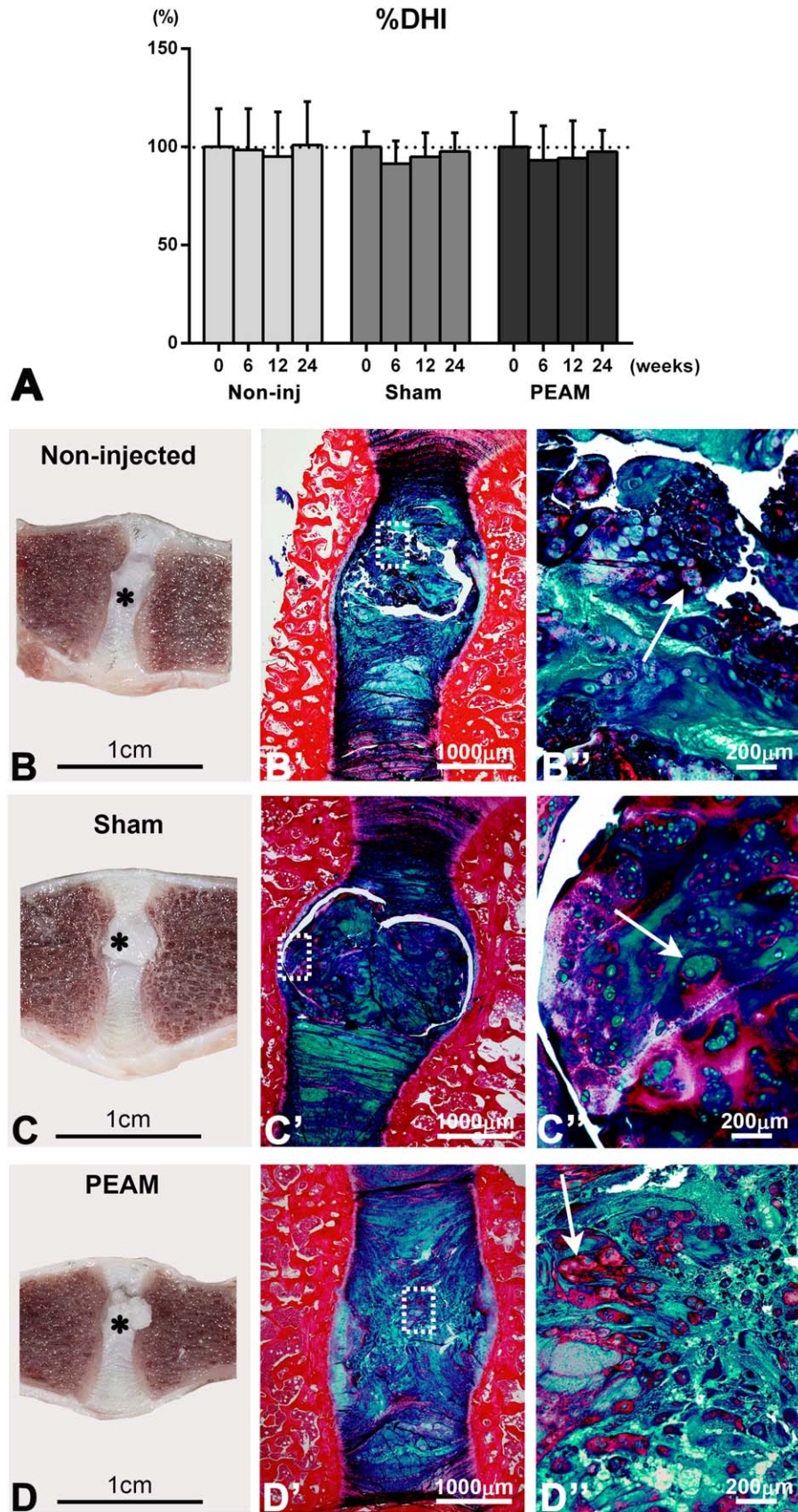


FIGURE 1. A. Change in disc height expressed as the percent disc height index compared with the pre-injection value (set at 100%) in non, sham, and PEAM-, injected canine IVDs at 6 months follow-up \pm standard deviation. B.–D. Representative macroscopical (B–D) and histopathological images (picosirius red/alcan blue stain) of noninjected (B'–B''), intradiscally injected (sham [C'–C''] and PEA microspheres (PEAMs; D'–D'')) canine IVDs at 6 months follow-up. B'', C'', D'' are magnifications of the squares in B', C', D', respectively. B–D. Nuclei pulposi (NPs) in all conditions had a bulging aspect (asterisk) because of the processing method and the tissue properties. Regardless of the treatment, at macroscopy a white opaque NP could be noticed in all IVDs, consistent with early IVD degeneration. Histopathologically, also regardless of the treatment, small size chondrocyte groups, consisting of 2–7 cells (arrow), within a mixture of collagen-rich (red stain) and glycosaminoglycans-rich (GAG; blue and green stain) extracellular matrix were observed in the NP of all IVDs.

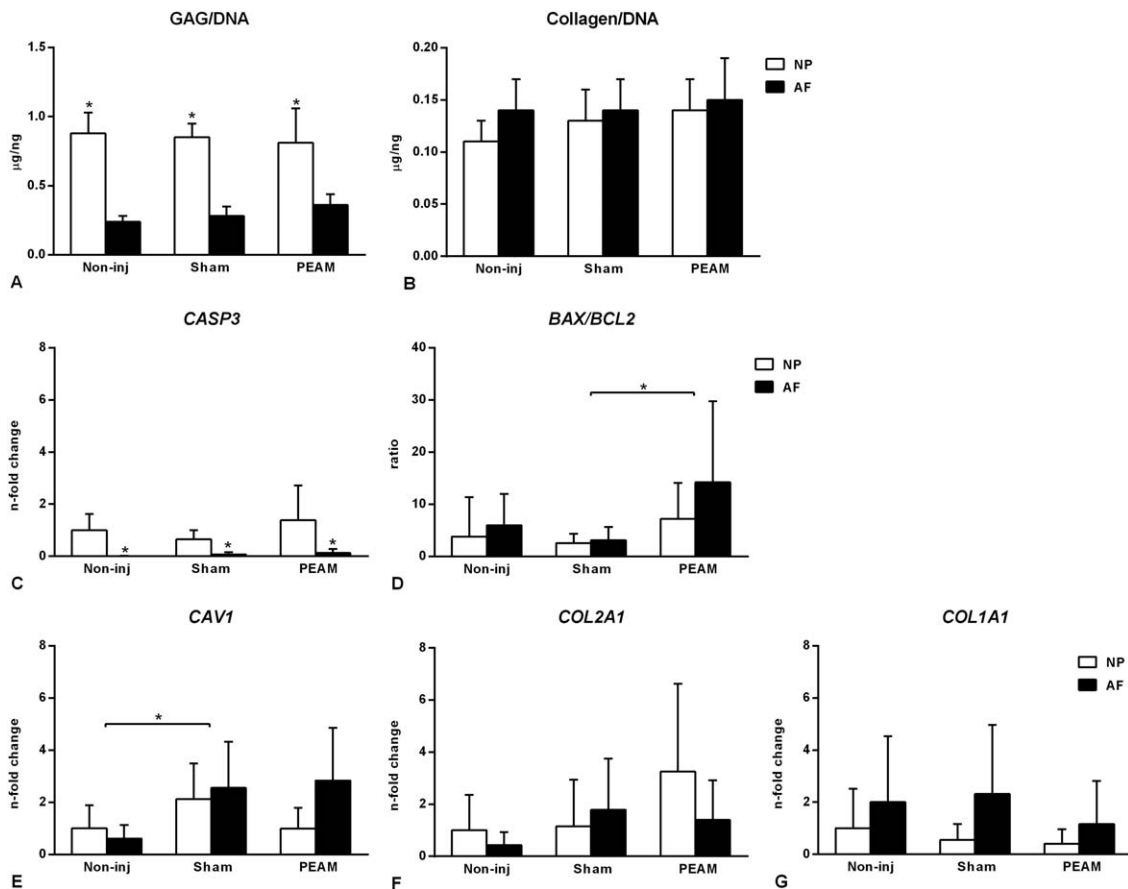


FIGURE 2. A–G. Relative gene expression levels in non, sham-, and PEAM-injected, canine IVDs at 6 months follow-up. The noninjected nuclei pulposi (NP) are set at 1. **A–C.** Gene expression levels of *COL2A1* (**A**) and *COL1A1* (**B**) were not significantly different between conditions, neither was collagen corrected for DNA (**C**). **D.** *CASP3* expression levels were significantly lower in the AF compared with the NP. **E.** Expression levels of *CAV1* were significantly higher in sham-injected IVDs (NP + AF) compared with noninjected control IVDs. **F.** In all conditions glycosaminoglycan (GAG) corrected for DNA were significantly higher in the NP compared with the AF. **G.** The PEAM-injected IVDs showed a significant higher *BAX/BCL2* ratio compared with the sham-injected IVDs. Data in **A**, **B**, **D**, and **E** are expressed as *n*-fold changes, in **C** and **F** as mean values, and in **G** as ratio \pm standard deviation. *Indicate significant difference at a 99% confidence level

collagen levels corrected for DNA were not different between conditions [Figure 2(A,B)]. In all conditions, GAG/DNA was significantly higher in the NP compared with the AF (M 0.55, SD 0.04; $CI_{99\%}$ 0.44–0.66).

Gene expression apoptotic and degenerative pathways and immunohistochemistry

Relative gene expression of *CASP3* in the AF was significantly lower (HR 0.21; $CI_{99\%}$ 0.07–0.66) than in the NP in all conditions and could be suggestive of a higher apoptotic rate in the NP [Figure 2(C)]. The *BAX/BCL2* ratio in the sham-injected IVDs (NP and AF) was significantly lower (HR 0.14; $CI_{99\%}$ 0.02–0.85) compared with the PEAMs-injected IVDs, indicative of an anti-apoptotic effect of the PEAMs [Figure 2(D)]. In addition, *CAV1* gene expression was significantly higher (HR 3.30; $CI_{99\%}$ 1.00–10.83) in sham-injected IVDs (NP and AF) compared with noninjected IVDs [Figure 2(E)]. None of the IVDs showed staining of cells with anti-caveolin-1 antibody in the NP and/or AF. Relative gene expression of anabolic (*ACAN*, *COL2A1* [Figure 2(F)], *COL1A1* [Figure 2(G)]), catabolic (*MMP13*), anti-catabolic (*TIMP1*),

and proliferative (*CCND1*) genes were not significantly different (Supporting Information 4). Gene expression of *ADAMTS5* was below detectable levels in the NP as well as the AF in all conditions.

DISCUSSION

In this study, intradiscal injection of a volume of 40 μ L through 26 and 27G needles induced no degenerative changes in a canine model predisposed to IVD degeneration at long-term (6 months) follow-up. Although sham-injected IVDs showed increased *CAV1* expression compared with noninjected IVDs, which may indicate increased cell senescence,³⁰ these findings were not supported by immunohistochemistry, biomolecular analysis of genes related to apoptosis, biochemical, and histopathological results.

A needle puncture has been described to alter mechanical properties by reducing pressure in the NP and/or damaging the AF, depending on the diameter of the needle. The rabbit annular stab model of induced IVD degeneration is based upon this concept.³¹ IVD degeneration has been observed when the ratio of needle diameter to disc height

exceeded 40%.¹⁵ With regard to injection volume, the NP can be considered as a confined space in which the hydrostatic pressure will increase if a substance is injected.¹⁸ In the caudal IVDs of rats, volume-dependent degenerative changes have been demonstrated after injection of phosphate buffered saline at a radiographic, biochemical, and histopathological level.¹⁹ Although the exact threshold volumes were not specified, injected volumes up to 66% (that is, 2 μL of 3.1 mm^3) of the total NP volume, showed no degenerative changes at short-term follow-up. Needle size diameters and injected volume applied in our study were well within the safety ranges described in literature, and induced no degenerative changes in canine IVDs predisposed to degeneration.

Furthermore, we showed a good cytocompatibility *in vitro* and biocompatibility of PEAs in rabbits. Only a slight foreign body reaction was seen after intramuscular implantation in rabbits. We hypothesized that intradiscal application of PEAs in the avascular IVD would be well accepted, in line with previous studies showing a moderate subcutaneous tissue response to a hydrogel that showed no response at all upon intradiscal injection.³² Furthermore, safe intravitreal application of PEA fibrils through a 26G needle was already shown by Kropp et al.¹³ Indeed, PEAMs were considered safe within a 6 months follow-up period, based on clinical signs, disc height index, T2 values, biomolecular and biochemical analyses, and IVD histopathology. The focal, mild granulomatous reaction described in one of the PEAM injected IVDs could have been a consequence of leakage of the PEAMs, the injection procedure itself, or it could have been a reaction consistent with the ongoing process of IVD degeneration.³³ The PEAMs-injected IVDs showed a significant higher *BAX/BCL2* ratio compared with the sham-injected IVDs, suggestive of an anti-apoptotic effect of the PEAMs. However, neither substance significantly affected this parameter compared with the noninjected controls, thus questioning the implications of this finding.

Several clinical trials are currently being performed, in which promising regenerative treatments, consisting of cell, gene, and protein therapies, are injected into the IVD (<http://clinicaltrials.gov>). In order to use PEAMs as a part of a regenerative therapy, effectuating sustained release of bioactive substances in the degenerative IVD, release profiles and degradation processes in the intradiscal environment need to be investigated in future. The stage of degeneration has been shown to be an important factor in the efficacy of treatment with cell-based therapies, which emphasizes the importance of the preclinical canine model that resembles the human situation.³⁴

CONCLUSION

In conclusion, we showed a good cytocompatibility *in vitro* and biocompatibility of PEAs in rabbits. Intradiscal injection of 40 μL of a sham condition through a 27G needle, and of PEA microspheres through a 26G, could be safely applied in this canine model predisposed to IVD degeneration without

accelerating degeneration over the course of 6 months. Hence, PEA microspheres are safe to use and form the basis for the development of regenerative strategies based on sustained release of bioactive substances in the degenerative IVD.

ACKNOWLEDGMENTS

This research forms part of the Project P2.01 IDiDAS of the research program of the BioMedical Materials institute, co-funded by the Dutch Ministry of Economic Affairs, Agriculture and Innovation. The financial contribution of the Dutch Arthritis Foundation is gratefully acknowledged (IDiDAS, LLP22 and LLP12). We would like to acknowledge Toxikon Corporation (Bedford, MA, USA) for performing the cytocompatibility tests *in vitro*, and the biocompatibility tests *in vivo*. Furthermore we would like to express our sincere appreciation to Saskia Plomp and Jeannette Wolfswinkel for their assistance in the laboratory.

REFERENCES

- Bergknut N, Rutges JP, Kranenburg HC, Smolders LA, Hagman R, Smidt HJ, Lagerstedt AS, Penning LC, Voorhout G, Hazewinkel HA, Grinwis GC, Creemers LB, Meij BP, Dhert WJ. The dog as an animal model for intervertebral disc degeneration? *Spine (Phila Pa 1976)* 2012;37:351–358.
- Roughley PJ. Biology of intervertebral disc aging and degeneration: Involvement of the extracellular matrix. *Spine (Phila Pa 1976)* 2004 ;29:2691–2699.
- Grunhagen T, Wilde G, Soukane DM, Shirazi-Adl SA, Urban JP. Nutrient supply and intervertebral disc metabolism. *J Bone Joint Surg Am* 2006;88(Suppl2):30–35.
- Putney SD, Burke PA. Improving protein therapeutics with sustained-release formulations. *Nat Biotechnol* 1998;16:153–157.
- DeFife KM, Grako K, Cruz-Aranda G, Price S, Chantung R, Macpherson K, Khoshabeh R, Gopalan S, Turnell WG. Poly(ester amide) co-polymers promote blood and tissue compatibility. *J Biomater Sci Polym Ed* 2009;20:1495–1511.
- Rodriguez-Galan A, Franco L, Puiggali J. Degradable poly(ester amide)s for biomedical applications. *Polymers* 2011;3:65–99.
- Guo K, Chu CC. Biodegradable and injectable paclitaxel-loaded poly(ester amide)s microspheres: Fabrication and characterization. *J Biomed Mater Res B Appl Biomater* 2009;89:491–500.
- Sun H, Meng F, Dias AA, Hendriks M, Feijen J, Zhong Z. Alpha-amino acid containing degradable polymers as functional biomaterials: Rational design, synthetic pathway, and biomedical applications. *Biomacromolecules* 2011 ;12:1937–1955.
- Ghaffar A, Draaisma GJ, Mihov G, Dias AA, Schoenmakers PJ, van der Wal S. Monitoring the *in vitro* enzyme-mediated degradation of degradable poly(ester amide) for controlled drug delivery by LC-ToF-MS. *Biomacromolecules* 2011 ;12:3243–3251.
- Mihov G, Draaisma G, Dias A, Turnell B, Gomurashvili Z. Degradable poly(esteramide)s: A novel platform for sustained drug delivery. *J Control Release* 2010 ;148:e46–e47.
- Lee SH, Szinai I, Carpenter K, Katsarava R, Jokhadze G, Chu CC, Huang Y, Verbeken E, Bramwell O, De Scheerder I, Hong MK. *In vivo* biocompatibility evaluation of stents coated with a new biodegradable elastomeric and functional polymer. *Coron Artery Dis* 2002;13:237–241.
- Webster M, Harding S, McClean D, Jaffe W, Ormiston J, Aitken A, Watson T. First-in-human evaluation of a sirolimus-eluting coronary stent on an integrated delivery system: The DIRECT study. *EuroIntervention* 2013 ;9:46–53.
- Kropp M, Morawa K, Mihov G, Salz A, Harmening N, Franken A, Kemp A, Dias A, Thies J, Johnen S, Thumann G. Biocompatibility of poly(esteramide) (PEA) microfibrils in ocular tissues. *Polymers* 2014;6:243–260.
- Andres-Guerrero V, Zong M, Ramsay E, Rojas B, Sarkhel S, Gallego B, de Hoz R, Ramirez AI, Salazar JJ, Trivino A, Ramirez

- JM, Del Amo EM, Cameron N, de-Las-Heras B, Urtti A, Mihov G, Dias A, Herrero-Vanrell R. Novel biodegradable polyesteramide microspheres for controlled drug delivery in ophthalmology. *J Control Release* 2015 ;211:105–117.
15. Elliott DM, Yerramalli CS, Beckstein JC, Boxberger JI, Johannessen W, Vresilovic EJ. The effect of relative needle diameter in puncture and sham injection animal models of degeneration. *Spine (Phila Pa 1976)* 2008;33:588–596.
 16. Wang JL, Tsai YC, Wang YH. The leakage pathway and effect of needle gauge on degree of disc injury post anular puncture: A comparative study using aged human and adolescent porcine discs. *Spine (Phila Pa 1976)* 2007 ;32:1809–1815.
 17. Masuda K, Aota Y, Muehleman C, Imai Y, Okuma M, Thonar EJ, Andersson GB, An HS. A novel rabbit model of mild, reproducible disc degeneration by an annulus needle puncture: Correlation between the degree of disc injury and radiological and histological appearances of disc degeneration. *Spine (Phila Pa 1976)* 2005; 30:5–14.
 18. Schechtman H, Robertson PA, Broom ND. Failure strength of the bovine caudal disc under internal hydrostatic pressure. *J Biomech* 2006;39:1401–1409.
 19. Mao HJ, Chen QX, Han B, Li FC, Feng J, Shi ZL, Lin M, Wang J. The effect of injection volume on disc degeneration in a rat tail model. *Spine (Phila Pa 1976)* 2011 ;36:E1062–E1069.
 20. Katsarava R, Beridze V, Arabuli N, Kharadze D, Chu C, Won C. Amino acid-based bioanalogous polymers. synthesis, and study of regular poly(ester amide)s based on bis (α -amino acid) α,ω -alkylene diesters, and aliphatic dicarboxylic acids. *J Polym Sci A Polym Chem* 1999;37:391–407.
 21. Roehm NW, Rodgers GH, Hatfield SM, Glasebrook AL. An improved colorimetric assay for cell proliferation and viability utilizing the tetrazolium salt XTT. *J Immunol Methods* 1991 ;142: 257–265.
 22. Willems N, Bach FC, Plomp SG, van Rijen MH, Wolfswinkel J, Grinwis GC, Bos C, Strijkers GJ, Dhert WJ, Meij BP, Creemers LB, Tryfonidou MA. Intradiscal application of rhBMP-7 does not induce regeneration in a canine model of spontaneous intervertebral disc degeneration. *Arthritis Res Ther* 2015 ;17:137.
 23. Kristensen HK. An improved method of decalcification. *Stain Technol* 1948;23:151–154.
 24. Bergknut N, Meij BP, Hagman R, de Nies KS, Rutges JP, Smolders LA, Creemers LB, Lagerstedt AS, Hazewinkel HA, Grinwis GC. Intervertebral disc disease in dogs - part 1: A new histological grading scheme for classification of intervertebral disc degeneration in dogs. *Vet J* 2013;195:156–163.
 25. Smolders LA, Meij BP, Onis D, Riemers FM, Bergknut N, Wubbolts R, Grinwis GC, Houweling M, Groot Koerkamp MJ, van Leenen D, Holstege FC, Hazewinkel HA, Creemers LB, Penning LC, Tryfonidou MA. Gene expression profiling of early intervertebral disc degeneration reveals a down-regulation of canonical wnt signaling and caveolin-1 expression: Implications for development of regenerative strategies. *Arthritis Res Ther* 2013;15:R23.
 26. Farndale RW, Sayers CA, Barrett AJ. A direct spectrophotometric microassay for sulfated glycosaminoglycans in cartilage cultures. *Connect Tissue Res* 1982;9:247–248.
 27. Neuman RE, Logan MA. The determination of hydroxyproline. *J Biol Chem* 1950;184:299–306.
 28. ISO 10993-5:2009 biological evaluation of medical devices. part 5: Tests for in vitro cytotoxicity; international organization for standardization: Geneva, Switzerland, 2009.
 29. Kranenburg HC, Meij BP, Onis D, van der Veen AJ, Saralidze K, Smolders LA, Huizinga JG, Knetsch ML, Luijten PR, Visser F, Voorhout G, Dhert WJ, Hazewinkel HA, Koole LH. Design, synthesis, imaging, and biomechanics of a softness-gradient hydrogel nucleus pulposus prosthesis in a canine lumbar spine model. *J Biomed Mater Res B Appl Biomater* 2012;100:2148–2155.
 30. Heathfield SK, Le Maitre CL, Hoyland JA. Caveolin-1 expression and stress-induced premature senescence in human intervertebral disc degeneration. *Arthritis Res Ther* 2008;10:R87.
 31. Sobajima S, Shimer AL, Chadderdon RC, Kompel JF, Kim JS, Gilbertson LG, Kang JD. Quantitative analysis of gene expression in a rabbit model of intervertebral disc degeneration by real-time polymerase chain reaction. *Spine J* 2005;5:14–23.
 32. Willems N, Yang H, Langelaan M, Tellegen A, Grinwis G, Kranenburg H, Riemers F, Plomp S, Craenmehr E, Dhert W, Papen-Butterhuis N, Meij B, Creemers L, Tryfonidou M. Biocompatibility and intradiscal application of celecoxib-loaded pNIPAAAM MgFe-LDH hydrogels in a canine spontaneous intervertebral disc degeneration model. *Arthritis Res Ther* 2015;17: 214
 33. Kranenburg HC, Grinwis GC, Bergknut N, Gahrman N, Voorhout G, Hazewinkel HA, Meij BP. Intervertebral disc disease in dogs—Part 2: Comparison of clinical, magnetic resonance imaging, and histological findings in 74 surgically treated dogs. *Vet J* 2013;195: 164–171.
 34. Ho G, Leung VY, Cheung KM, Chan D. Effect of severity of intervertebral disc injury on mesenchymal stem cell-based regeneration. *Connect Tissue Res* 2008;49:15–21.